Temperature-dependent Raman spectra of $HoMn_2O_5$ and $TbMn_2O_5$

B. Mihailova,[1] M. M. Gospodinov,[2] B. Güttler,[3] F. Yen,[4] A. P. Litvinchuk,[4] and M. N. Iliev[4]
[1]*Central Laboratory of Mineralogy and Crystallography, Bulgarian Academy of Sciences, 1113 Sofia, Bulgaria*
[2]*Institute of Solid State Physics, Bulgarian Academy of Sciences, 1784 Sofia, Bulgaria*
[3]*Physikalisch-Technische Bundesanstalt, 38116 Braunschweig, Germany*
[4]*Texas Center for Superconductivity and Advanced Materials, and Department of Physics, University of Houston, Houston, Texas 77204-5002, USA*
(Received 1 November 2004; revised manuscript received 22 December 2004; published 2 May 2005)

The polarized Raman spectra of $HoMn_2O_5$ and $TbMn_2O_5$ are reported and discussed. Most of the Raman lines corresponding to Γ-point Raman modes ($13A_g+13B_{1g}+11B_{2g}+11B_{3g}$) have been observed. The temperature dependence of the $HoMn_2O_5$ spectra provides no evidence for phonon anomalies associated with magnetic and ferroelectric transitions below 50 K.

DOI: 10.1103/PhysRevB.71.172301 PACS number(s): 78.30.Hv, 63.20.Dj, 72.80.Ga, 77.84.−s

Introduction. The increased interest to the RMn_2O_5 (R = rare earth or Y) is motivated to a great extent by the observation of cross-correlation between magnetic and dielectric properties of this family of oxides.[1–4] All materials are isostructural (space group *Pbam*, No.55, $Z=4$)[5,6] and contain infinite chains of Mn^{4+} octahedra along c direction linked together by Mn^{3+} pyramids (Fig. 1). RMn_2O_5 exhibit a helical antiferromagnetic (AFM) ordering below the Néel temperature of 40–45 K and ferroelectric (FE) ordering at the same or somewhat lower temperature.[1–4,7–12] Further lowering of temperature reveals a set of consecutive AFM and FE phase transitions associated with change of the AFM commensurate ordering of Mn subsystem into an "incommensurate" one and AFM ordering of the R^{3+} moments.[2,3,11–13]

The mechanism of spontaneous polarization is not known at present. Most diffraction experiments have not provided direct evidence of lattice distortions around FE transitions. The only exception is the work of Polyakov *et al.*[11] on the neutron diffraction from $EuMn_2O_5$ where polar displacements of Mn^{3+} ions along the a axis, due to $Pbam \rightarrow P2_1am$ structural transition have been reported at the concomitant AFM and FE transitions around 40 K. A second $P2_1am \rightarrow P1a1$ structural transition resulting in polar shifts of the Mn^{4+} along the c axis has been observed at $T \approx 22$ K.

Although a considerable number of reports have been accumulated on the structural, magnetic, and dielectric properties of RMn_2O_5, there are scarce data on electronic and optical properties of these materials. In particular, neither theoretical nor experimental results on the phonons are available so far. In this work we present the polarized Raman spectra of $HoMn_2O_5$ and their variations with temperature between 10 and 300 K. The spectra of $TbMn_2O_5$ at 300 K are also reported. Most of the Raman lines of A_g, B_{1g}, B_{2g}, and B_{3g} symmetry expected for the *Pbam* structure have been observed. The temperature dependence of the $HoMn_2O_5$ spectra exhibits no anomalies that may be associated with AFM or FE ordering.

Samples and experimental. Polycrystalline $HoMn_2O_5$ and $TbMn_2O_5$ were sintered by solid-state reaction of stoichiometric amounts of Ho_2O_3, Tb_2O_3, and MnO_2, and further annealed for 48 h at 1150 °C in oxygen atmosphere. Single crystals of $HoMn_2O_5$ and $TbMn_2O_5$ were grown by the high temperature solution growth method using $PbO—PbF_2—B_2O_3$ flux ($PbO:PbF_2:B_2O_3$ = 0.75:0.24:0.01 for $HoMn_2O_5$ and 0.87: 0.12: 0.01 for $TbMn_2O_5$, respectively). The flux was mixed with $HoMn_2O_5$ powder in a 10:1 ratio or with $TbMn_2O_5$ powder in a 7:1 ratio and annealed in platinum crucible at 1225 °C for 48 h in air. After annealing the temperature was decreased to 950 °C at a rate of 0.5 °C/h for $HoMn_2O_5$ and to 1000 °C at a rate of 1 °C/h for $TbMn_2O_5$. The flux was decanted and well-shaped parallelepipedlike crystals of typical dimensions $4\times4\times2$ mm^3 were removed from the bottom of the Pt crucible.

The crystallographic directions and lattice parameters were determined using a GADDS x-ray diffractometer (Brucker). The values of $a=7.26$ Å, $b=8.47$ Å, and $c=5.67$ Å for $HoMn_2O_5$, and $a=7.32$ Å, $b=8.52$ Å, $c=5.68$ Å for $TbMn_2O_5$ are close to those known from the literature.[5,6]

The temperature dependence of the heat capacity C_p of the $HoMn_2O_5$ crystal used in Raman experiments was measured employing the Physical Property Measurement System

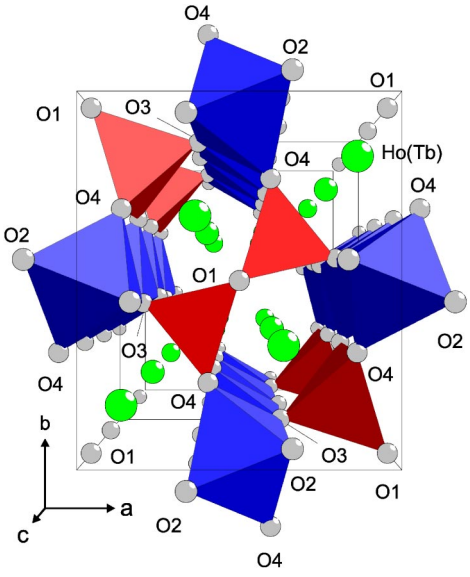

FIG. 1. Structure of RMn_2O_5.

(Quantum Design). The dielectric constant ϵ of the same crystal was measured at 100 kHz using the HP 4285A LCZ meter. Data were collected upon cooling and heating cycles.

The temperature dependences shown in Fig. 2 are in perfect agreement with those recently reported by Hur *et al.*[2] $HoMn_2O_5$ undergoes several magnetic and ferroelectric phase transitions with decreasing temperature. At $T_N = 43.5$ K long-range antiferromagnetic order of the Mn^{3+}/Mn^{4+} sets in, as clearly indicated by the first peak of the heat capacity, C_p [Fig. 2(a)]. The second sharp peak of C_p at $T_C = 39$ K is because of a phase transition into a ferroelectric state, also indicated by the peak of the dielectric constant, ϵ [Fig. 2(b)]. With further decreasing temperature C_p and ϵ exhibit a distinct, steplike increase at 20 K, the temperature at which a sudden increase of the ferroelectric polarization was observed.[2] This transition was ascribed to the appearance of an incommensurate magnetic order below 20 K. Close to 15 K a sharp increase of ϵ with a clear thermal hysteresis is observed [Fig. 2(b)]. The origin of this anomaly is not yet understood. It could be related to a possible lock-in of the temperature dependent incommensurate wave vector for magnetic order into a *T*-independent constant value, as e.g., observed in some orthorhombic rare-earth $RMnO_3$.[14]

The Raman spectra were measured in a backward-scattering configuration with 514.5 nm excitation using a single spectrometer Jobin-Yvon HR640 (spectral resolution 0.5 cm^{-1}), equipped with microscope, notch filter and liquid-nitrogen-cooled CCD detector. For measurements between 10 and 300 K the samples were cooled in a Microstat^{He} (Oxford Instruments) optical cryostat and extremely low laser power of 0.1 mW was used to avoid local heating. The Raman line parameters were determined using the fitting program of the GRAMS AI software.

The faces of the as-grown crystals were parallel to the (100), (010), (001), or (110) planes, which allowed one to obtain the spectra in all exact scattering configurations: *xx*, *yy*, *zz*, *xy*, *xz*, and *yz*. The first and second letters in these notations denote the polarizations of the incident and scattered light, respectively.

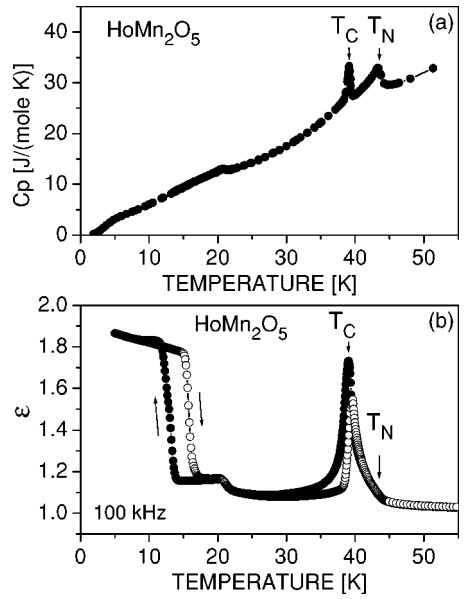

FIG. 2. Temperature dependence of (a) heat capacity C_p and (b) dielectric function of $HoMn_2O_5$. The arrows indicate the antiferromagnetic transition at $T_N = 43.5$ K and the ferroelectric transition at $T_C = 39$ K.

Γ-*point Raman active phonons in* RMn_2O_5. The site-symmetry analysis[15] of the *Pbam* structure of RMn_2O_5 (see Table I) shows that out of a total 96 Γ-point phonon modes 48 $(13A_g + 13B_{1g} + 11B_{2g} + 11B_{3g})$ are Raman active, 36 $(8B_{1u} + 14B_{2u} + 14B_{3u})$ are infrared (IR) active, 9 $(9A_u)$ are silent, and 3 $(B_{1u} + B_{2u} + B_{3u})$ are acoustical modes.

TABLE I. Wyckoff notations, atomic site symmetries, and irreducible representations (Γ-point phonon modes) for RMn_2O_5 (space group *Pbam*, No. 55, $Z = 4$).

Atom	Wickoff notation	Site symmetry	Γ-point phonon modes
Ho(Tb)	4g	C_s^{xy}	
			$2A_g + A_u + 2B_{1g} + B_{1u} + B_{2g} + 2B_{2u} + B_{3g} + 2B_{3u}$
Mn1	4f	C_2^z	$A_g + A_u + B_{1g} + B_{1u} + 2B_{2g} + 2B_{2u} + 2B_{3g} + 2B_{3u}$
Mn2	4h	C_s^{xy}	$2A_g + A_u + 2B_{1g} + B_{1u} + B_{2g} + 2B_{2u} + B_{3g} + 2B_{3u}$
O1	4e	C_2^z	$A_g + A_u + B_{1g} + B_{1u} + 2B_{2g} + 2B_{2u} + 2B_{3g} + 2B_{3u}$
O2	4g	C_s^{xy}	$2A_g + A_u + 2B_{1g} + B_{1u} + B_{2g} + 2B_{2u} + B_{3g} + 2B_{3u}$
O3	4h	C_s^{xy}	$2A_g + A_u + 2B_{1g} + B_{1u} + B_{2g} + 2B_{2u} + B_{3g} + 2B_{3u}$
O4	8i	C_1	$3A_g + 3A_u + 3B_{1g} + 3B_{1u} + 3B_{2g} + 3B_{2u} + 3B_{3g} + 3B_{3u}$

Modes classification

$\Gamma_{Raman} = 13A_g + 13B_{1g} + 11B_{2g} + 11B_{3g}$ $\quad \Gamma_{IR} = 8B_{1u} + 14B_{2u} + 14B_{3u}$ $\quad \Gamma_{Acoustic} = B_{1u} + B_{2u} + B_{3u}$

Raman tensors

$$A_g \rightarrow \begin{bmatrix} a & 0 & 0 \\ 0 & b & 0 \\ 0 & 0 & c \end{bmatrix} \quad B_{1g} \rightarrow \begin{bmatrix} 0 & d & 0 \\ d & 0 & 0 \\ 0 & 0 & 0 \end{bmatrix} \quad B_{2g} \rightarrow \begin{bmatrix} 0 & 0 & e \\ 0 & 0 & 0 \\ e & 0 & 0 \end{bmatrix} \quad B_{3g} \rightarrow \begin{bmatrix} 0 & 0 & 0 \\ 0 & 0 & f \\ 0 & f & 0 \end{bmatrix}$$

The A_g modes are expected to appear in the parallel *xx*, *yy*, and *zz* scattering configurations and should not be seen in the crossed *xy*, *xz*, and *yz* configurations. The B_{1g}, B_{2g}, and B_{3g} modes are allowed, respectively, in *xy*, *xz*, and *yz* configurations.

Results and discussion. Figure 3 shows the polarized Raman spectra of $HoMn_2O_5$ at 10 and 300 K and of $TbMn_2O_5$ at 300 K. Twelve of 13 expected lines of A_g symmetry, as well as 9 of 13 B_{1g}, 8 of 11 B_{2g}, and 8 of 11 B_{3g} lines are experimentally observed. Their positions are summarized in Table II. The missing modes are of very low intensity or superimposed or out of the spectral range (<100 cm^{-1}) of our Raman setup. An assignment of the Raman lines to definite modes is not possible at present. On the basis of mass and bond lengths considerations, however, it is reasonable to accept that the lines at >300 cm^{-1} correspond to modes involving mainly stretching and bending vibrations of light oxygen atoms, whereas those at lower frequencies involve motions of heavier Mn and Ho(Tb) atoms. Most of the lines in the low-frequency range are extremely sharp, indicating weak anharmonicity.

Figure 4 shows the temperature dependence of the position of most pronounced A_g and B_{2g} lines of $HoMn_2O_5$ between 7 and 150 K. Compared to other transition metal oxides, frequency shifts are relatively small. The temperature range below 50 K is of particular interest as it contains both the Neél temperature $T_N=43.5$ K and the temperature of ferroelectric ordering $T_C=39$ K. From symmetry considerations one expects that the $Pbam \rightarrow P2_1am$ structural transition will result in appearance of additional Raman lines because in the less symmetric $P2_1am$ structure all optical phonon modes are Raman allowed. Although the "soft" mode(s) associated with the FE transition is(are) out of the spectral range of our setup ($\omega_{soft}<100$ cm^{-1}), activation of other modes at higher frequencies and small shifts of existing modes may be expected. Figure 5 shows the variations with *T* of the $x'x'$ (A_g+B_{1g}) spectra between 7 and 60 K and *xz* (B_{2g}) spectra between 9 and 100 K. Although most lines exhibit "normal" hardening with lowering temperature, the B_{2g} line near 514 cm^{-1} "softens" below 80 K [Fig. 4(e)]. There are no indications, however, for anomalies of the phonon line parameters near T_N or T_C or appearance of new lines at low temperatures.

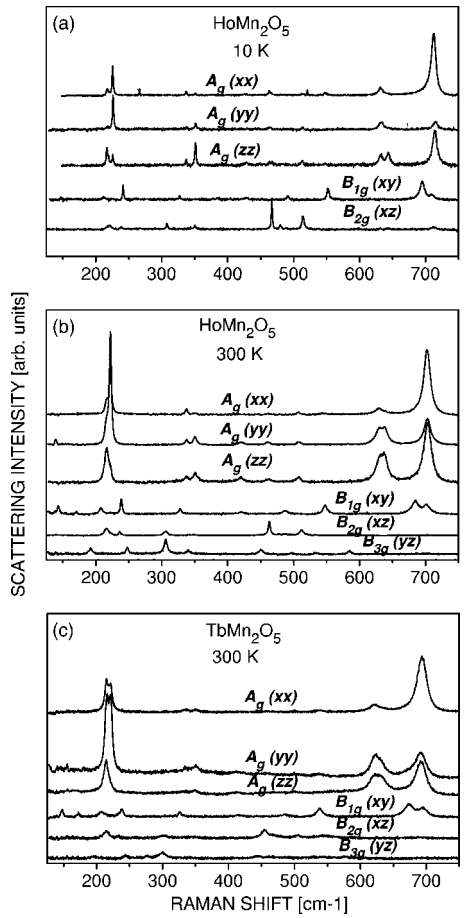

FIG. 3. Polarized Raman spectra of (a) $HoMn_2O_5$ at 10 K, (b) $HoMn_2O_5$ at 300 K, and (c) $TbMn_2O_5$ at 300 K.

TABLE II. Experimentally observed phonon mode frequencies (in cm^{-1}) for $HoMn_2O_5$ and $TbMn_2O_5$.

A_g Modes		B_{1g} Modes		B_{2g} Modes		B_{3g} Modes	
$HoMn_2O_5$ 10/300 K	$TbMn_2O_5$ 300 K	$HoMn_2O_5$ 10/300 K	$TbMn_2O_5$ 300 K	$HoMn_2O_5$ 10/300 K	$TbMn_2O_5$ 300 K	$HoMn_2O_5$ 10/300 K	$TbMn_2O_5$ 300 K
217/216	215	147/143	148	220/216	214	/192	195
219/		/170	172	238/236	232	/247	244
226/222	221	212/207	208	308/306	301	/306	299
337/337	334	241/239	237	467/463	455	/340	
351/351	350	327/327	326	480/	470	/451	442
428/420	412	429/420	416	489/		/497	
464/462		491/487	485	513/512	505	/534	540
513/508	500	552/547	538	598/594		/584	577
547/543	537	697/684	673				
633/630	621	709/702	695				
644/639	631						
717/703	693						

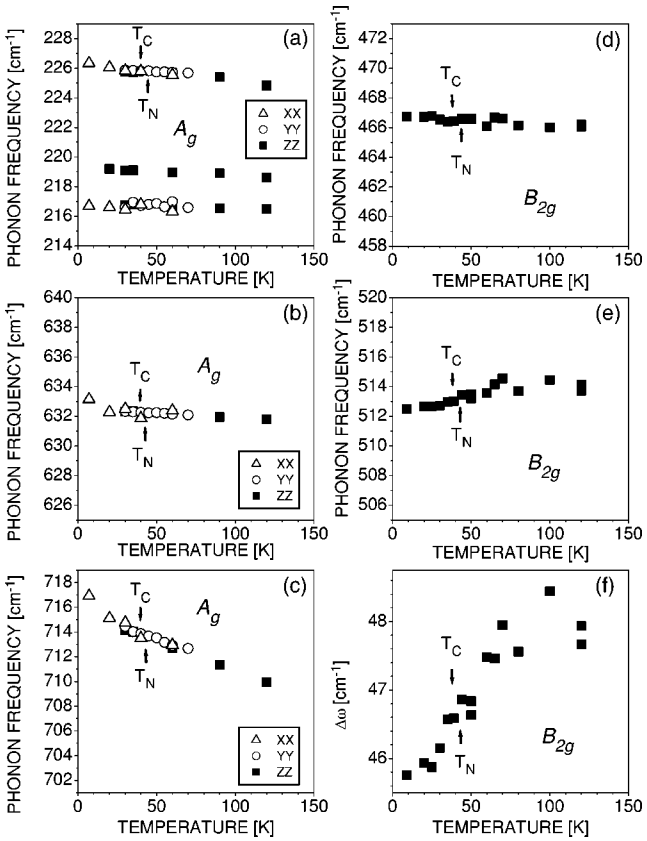

FIG. 4. Temperature dependence of the positions of most pronounced A_g (a–c) and B_{2g} (d,e) Raman lines in $HoMn_2O_5$. (e) Shows the temperature dependence of the difference between the positions of the B_{2g} lines near 513 and 566 cm^{-1}. No anomaly is observed near T_N and T_C.

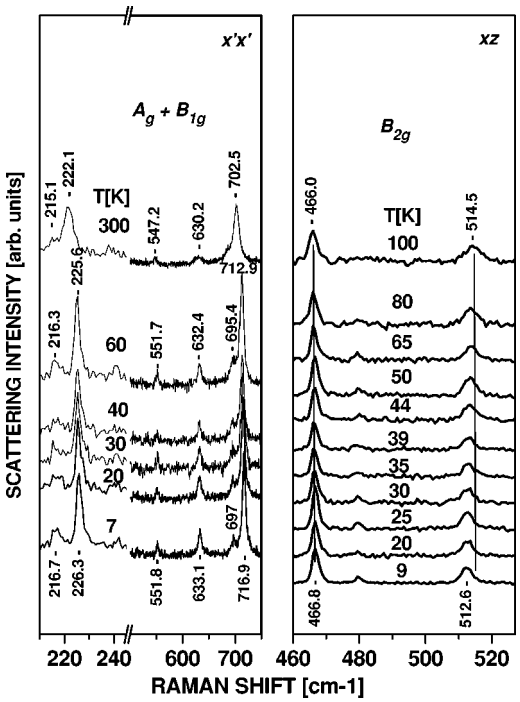

FIG. 5. Temperature variations of the $x'x'$ (A_g+B_{1g} spectra of $HoMn_2O_5$ between 7 and 300 K and xz (B_{2g}) spectra between 9 and 100 K. The phonon parameters exhibit no detectable anomaly related to antiferromagnetic and/or ferroelectric ordering.

It is worth noting here, that the sharpness of the Raman lines and the resolution of our spectrometer allowed to reduce to <0.5 cm^{-1} the error in determining the changes with temperature of the Raman line position. For phonon frequencies higher than 200 cm^{-1} relative changes as small as 2.5×10^{-3} could reliably be detected. Such a high sensitivity allows detection of relatively weak structural changes. Indeed, in a rough approximation the vibrational frequency of a phonon mode involving vibrations of mainly one type of atoms is determined by the relation $\omega^2=kR^{-3}$, where k is the force constant and R is the distance between the atom and its nearest neighbor(s). With respect to the relative changes of the bond length, the latter relation can be rewritten as $|\Delta R/R|=2/3|(\Delta\omega/\omega)|$. As the bond lengths in $RMnO_3$ are of the order of 2 Å, changes of bond lengths larger than 0.003 Å could easily be detected spectroscopically by line position analysis. Our results do not provide evidence for such changes although the detection limit of 0.003 Å is comparable and even smaller than the displacements of Mn^{3+} ($\approx$0.005 Å at T_N and $\approx$0.007 Å at T_C) and Mn^{+4} ($\approx$0.004 Å at T_N and $\approx$0.045 Å at T_C) reported for $EuMn_2O_5$ from neutron-scattering experiments.[11]

Conclusions. The polarized Raman spectra of isostructural $HoMn_2O_5$ and $TbMn_2O_5$ were measured between 7 and 300 K. Most of the Raman lines corresponding to the Γ-point phonon modes of A_g, B_{1g}, B_{2g}, and B_{3g} were observed. The temperature dependence of the A_g spectra provides no evidence for anomalies associated with magnetic and/or ferroelectric ordering.

Acknowledgments. This work was supported in part by the State of Texas through the Texas Center for Superconductivity and Advanced Materials, by the Alexander von Humboldt Foundation (Bonn, Germany), and by the Bulgarian National Research Fund (Project F-1207).

[1] S. Kato *et al.*, Ferroelectrics **203**, 323 (1997).
[2] N. Hur *et al.*, Phys. Rev. Lett. **93**, 107207 (2004).
[3] D. Higashiyama, N. Kida, S. Miyasaka, T. Arima, and Y. Tokura, cond-mat/0405571 (unpublished).
[4] E. Golovenchits and V. Sanina, J. Phys.: Condens. Matter **16**, 4325 (2004).
[5] J. A. Alonso *et al.*, J. Phys.: Condens. Matter **9**, 8515 (1997).
[6] I. Kagomiya *et al.*, Ferroelectrics **280**, 131 (2002).
[7] V. A. Sanina *et al.*, Sov. Phys. Solid State **30**, 1736 (1988).
[8] C. Wilkinson *et al.*, J. Phys. C **14**, 1671 (1981).
[9] A. Inomata and K. Kohn, J. Phys.: Condens. Matter **8**, 2673 (1996).
[10] S. Matsumoto *et al.*, Ferroelectrics **286**, 185 (2003).
[11] V. Polyakov *et al.*, Physica B **297**, 208 (2001).
[12] S. Kobayashi *et al.*, J. Phys. Soc. Jpn. **73**, 1593 (2004).
[13] I. Kagomiya *et al.*, J. Phys. Soc. Jpn. **70**, 145 (2001).
[14] T. Goto *et al.*, Phys. Rev. Lett. **92**, 257201 (2004).
[15] D. L. Rousseau *et al.*, J. Raman Spectrosc. **10**, 253 (1981).